

## Article

# Improved Understanding of Flash Drought from a Comparative Analysis of Drought with Different Intensification Rates

Jiaqi Han <sup>1,2</sup>, Jiahua Zhang <sup>1,2,\*</sup> , Shanshan Yang <sup>3</sup>  and Ayalkibet M. Seka <sup>1,2</sup> 

<sup>1</sup> Key Laboratory of Digital Earth Science, Aerospace Information Research Institute, Chinese Academy of Sciences, Beijing 100094, China

<sup>2</sup> College of Earth and Planetary Sciences, University of Chinese Academy of Sciences, Beijing 100049, China

<sup>3</sup> Research Center for Remote Sensing Information and Digital Earth, College of Computer Science and Technology, Qingdao University, Qingdao 266071, China

\* Correspondence: zhangjh@radi.ac.cn

**Abstract:** The rapid intensification of drought, commonly known as flash drought, has recently drawn widespread attention from researchers. However, how the characteristics and drivers, as well as the ecological impacts of rapidly intensified droughts, differ from those of slowly intensified ones still remains unclear over the globe. To this end, we defined three types of droughts based on the root zone soil moisture (RZSM) decline rates, flash droughts, general droughts, and creep droughts, and then implemented a comparative analysis between them across the globe and the 26 Intergovernmental Panel on Climate Change Special Report on Extremes (IPCC-SREX) regions. The ensemble of RZSM from multiple reanalysis datasets was used to reduce the uncertainties. According to the frequency analysis, our findings suggest that flash droughts contributed to the majority of drought events during 1980–2019, indicating the prevalence of rapid transition from an energy-limited to a water-limited condition in most of the regions. The comparative results of vegetation responses show that flash droughts are more likely to happen in the growing season, leading to faster but relatively minor vegetation deterioration compared to the slowly intensified ones. By analyzing the precipitation and temperature anomalies in the month of drought onset, we found the role of temperature (precipitation) on drought intensification can be generalized as the warmer (drier) the climate is or the faster the drought intensifies, but the main driving forces vary by region. Unlike temperature dominating in midwestern Eurasia and northern high latitudes, precipitation plays a prominent role in the monsoon regions. However, the temperature is expected to be the decisive driver in the warming future, given its monotonically increased contribution over the past four decades.

**Keywords:** trend; vegetation response; global warming; SREX; soil moisture



**Citation:** Han, J.; Zhang, J.; Yang, S.; Seka, A.M. Improved Understanding of Flash Drought from a Comparative Analysis of Drought with Different Intensification Rates. *Remote Sens.* **2023**, *15*, 2049. <https://doi.org/10.3390/rs15082049>

Academic Editor: Xianjun Hao

Received: 19 February 2023

Revised: 26 March 2023

Accepted: 28 March 2023

Published: 12 April 2023



**Copyright:** © 2023 by the authors. Licensee MDPI, Basel, Switzerland. This article is an open access article distributed under the terms and conditions of the Creative Commons Attribution (CC BY) license (<https://creativecommons.org/licenses/by/4.0/>).

## 1. Introduction

Imbalanced water budgets on the land surface can create risks of extreme climate hazards, such as floods or droughts. Compared to floods, droughts have attracted more attention from researchers because of their higher occurrence, wider impacted areas, and severer losses. What is even more different is that drought has traditionally been considered a slow-onset phenomenon, usually taking several months or even years to reach its maximum intensity. However, recent studies have found that some droughts could develop rapidly in a short period of time, like floods, which are called “flash droughts” [1,2]; for example, the 2013 southern China drought [3], the 2017 northern US drought [4], and the 2018 southern Australia drought [5].

Since rapid intensification has become a widely accepted criterion for detecting flash drought [6], case studies and regional analyses on the spatial distribution and temporal trends of flash drought occurrence have been accomplished by kinds of scientific literature [7–11]. However, there is still a lack of consensus on flash drought hotspots and trends

because of the uncertainties associated with indicators and datasets [12–14]. Furthermore, in terms of the mechanism of flash drought, the key role of precipitation deficit and high temperature has been emphasized by several studies by analyzing how variables evolve before and during drought [5,15–18]. As a result, two distinct mechanisms were revealed, and two types of flash drought, precipitation deficit flash drought and heat wave flash drought, were categorized accordingly [19–22]. However, these separate analyses that only focus on the rapidly intensified ones of drought events may not sufficiently reveal the potential effects of precipitation and temperature in triggering rapid intensification, as the neglected ones with a slow onset may also be accompanied by equivalent precipitation or temperature anomalies. More importantly, regional differences in the role of precipitation and temperature are still unclear across the globe.

Therefore, this study aims to implement a comparative analysis between droughts with different intensification rates on a global scale. Specifically, we chose soil moisture to identify drought conditions and then extracted three types of droughts from the total drought events as “flash drought”, “general drought”, and “creep drought”. Multiple reanalysis datasets, including the European Center for Medium-Range Weather Forecasts Reanalysis 5 (ERA5), the Modern-Era Retrospective Analysis for Research and Applications Version 2 (MERRA2), the Climate Forecast System Reanalysis (CFSR), and the Japanese 55-year Reanalysis (JRA-55) were selected to constrain the uncertainties by the ensemble approach. We focus on differences in drought characteristics across the 26 Intergovernmental Panel on Climate Change Special Report on Extremes (IPCC-SREX) regions. Our goals are:

- (1) Identify the global hotspots and trends of drought with different intensification rates in the absence of consensus on flash drought characteristics;
- (2) Explore the difference in vegetation response to drought intensification rate;
- (3) Investigate the role of precipitation and temperature in affecting the drought intensification rate and their regional difference across the globe.

## 2. Materials and Methods

### 2.1. Study Area

The IPCC-SREX divides the world into 26 regions based on various factors, such as climate, geography, ecosystems, and socio-economic factors (Figure 1). In this study, we chose the 26 IPCC-SREX regions to explore the regional difference in drought characteristics.

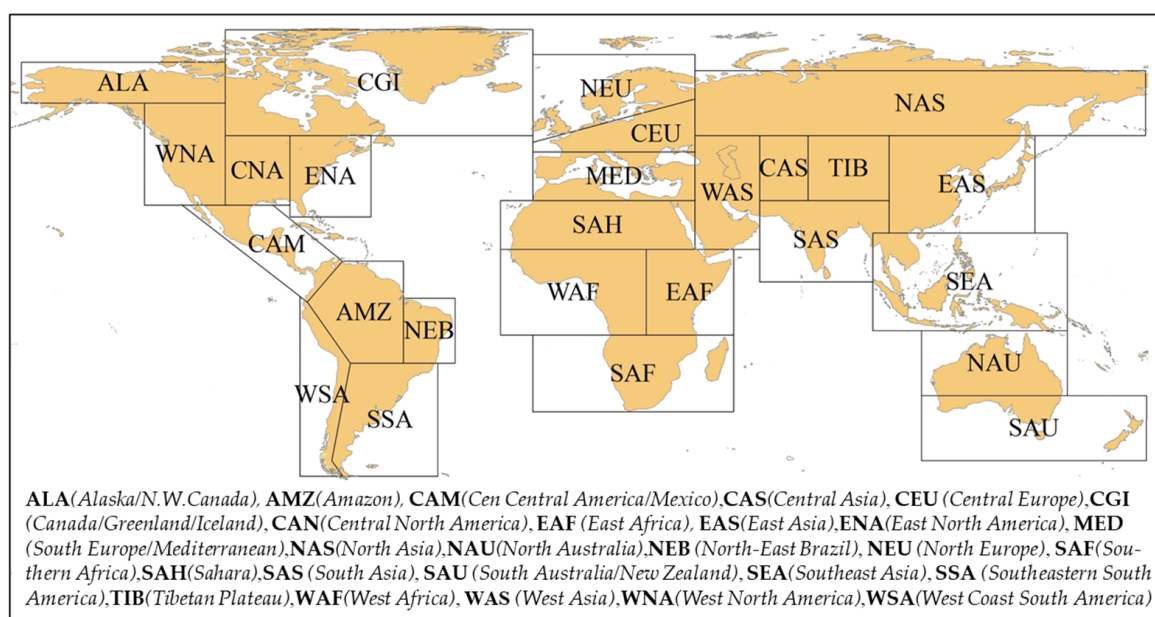


**Figure 1.** The global division scheme of the 26 IPCC-SREX.

## 2.2. Materials

### 2.2.1. Root Zone Soil Moisture (RZSM)

Global daily RZSM was obtained from the widely used ERA5, MERRA2, CFSR, and JRA-55 reanalysis datasets, which represent state-of-the-art products. We selected only the middle layer of RZSM data, and the research period spanned from 1980 to 2019 for all reanalysis products except for CFSR, where we used version 2 (CFSR2) to fill the gap of the last nine years. In addition to RZSM, we selected evapotranspiration (ET) and potential evaporation (PET) variables from the four reanalysis data to calculate the evapotranspiration stress ratio (ESR, calculated as evaporation/potential evaporation), which is another common indicator in flash drought identification. For datasets that do not provide potential evaporation, such as MERRA2 and JRA55, we downloaded the relevant variables required by Penman's formula for calculating PET, including wind speed, air pressure, net radiation, air temperature, dew point temperature, relative humidity, etc. Since CFSR does not provide an evaporation product, we chose latent heat flux for conversion. The ET and PET data were only used to evaluate the performance of RZSM and the ESR in the four reanalysis datasets and do not belong to the main analysis. Table 1 provides the characteristics of all the reanalysis variables.

We first averaged the hourly values daily and resampled the datasets to a  $0.5^\circ \times 0.5^\circ$  resolution using bilinear interpolation. Note that soil moisture in CFSR and JRA-55 is represented as relative humidity (%); therefore, we used the field capacity data to transfer them to volume soil moisture ( $\text{m}^3 \text{m}^{-3}$ ). Field capacity data were obtained from International Geosphere–Biosphere Program Data and Information System (IGBP-DIS) at <https://daac.ornl.gov/SOILS/guides/IGBP-DIS.html> (accessed on 27 March 2023). All the datasets were further composited to a temporal resolution of five days (pentad); thus, 73 pentads for each year and a total of 2920 pentads for the 40 years were obtained. Finally, the average ensemble dataset was developed to reduce the uncertainties among the four reanalysis datasets.

**Table 1.** The detail of reanalysis data used in the study.

|                                 | Variable                            | Unit                             | Temporal Resolution | Spatial Resolution             | Source  |
|---------------------------------|-------------------------------------|----------------------------------|---------------------|--------------------------------|---|
| ERA5                            | RZSM (28–100 cm)                    | $\text{m}^3 \text{m}^{-3}$       | hourly              | $0.25^\circ \times 0.25^\circ$ | <a href="https://cds.climate.copernicus.eu/cdsapp#!/home">https://cds.climate.copernicus.eu/cdsapp#!/home</a> (accessed on 27 March 2023)         |
|                                 | ET and PET                          | m                                |                     |                                |   |
| MERRA2                          | RZSM (0–100 cm)                     | $\text{m}^3 \text{m}^{-3}$       | hourly              | $0.5^\circ \times 0.625^\circ$ | <a href="https://disc.gsfc.nasa.gov/datasets?project=MERRA-2">https://disc.gsfc.nasa.gov/datasets?project=MERRA-2</a> (accessed on 27 March 2023) |
|                                 | ET                                  | $\text{kg m}^{-2} \text{s}^{-1}$ |                     |                                |   |
|                                 | 2 m temperature and dew temperature | K                                |                     |                                |   |
|                                 | Surface pressure                    | Pa                               | daily               |                                |   |
| 2 m northward and eastward wind | $\text{m s}^{-1}$                   |                                  |                     |                                |   |
|                                 | Net longwave and shortwave          | $\text{W m}^{-2}$                |                     |                                |   |
| CFSR/CFSR2                      | RZSM (40–100 cm)                    | %                                | 6-hourly            | $0.5^\circ \times 0.5^\circ$   | <a href="https://rda.ucar.edu/datasets/ds094.0/">https://rda.ucar.edu/datasets/ds094.0/</a> (accessed on 27 March 2023)                           |
|                                 | Potential water evaporation flux    | $\text{W m}^{-2}$                |                     |                                |   |
|                                 | Latent heat flux                    |                                  |                     |                                |   |

Table 1. Cont.

|   | Variable                         | Unit              | Temporal Resolution | Spatial Resolution             | Source   |
|---|----------------------------------|-------------------|---------------------|--------------------------------|--|
| JRA55                                   | RZSM (0.02 cm–148 cm)            | %                 | 6-hourly            |                                |  |
|   | ET                               | $\text{W m}^{-2}$ | 3-hourly            |                                |  |
|   | Relative humidity                | %                 |                     |                                | <a href="https://rda.ucar.edu/datasets/ds628.0/">https://rda.ucar.edu/datasets/ds628.0/</a><br>(accessed on 27 March 2023) |
|   | 2 m temperature                  | K                 | 6-hourly            | $0.56^\circ \times 0.56^\circ$ |  |
|   | 10 m northward and eastward wind | $\text{m s}^{-1}$ |                     |                                |  |
|   | Surface pressure                 | Pa                |                     |                                |  |
| Downward and upward long-wave radiation | $\text{W m}^{-2}$                |                   | 3-hourly            |                                |  |
| Downward and upward solar radiation     |                                  |                   |                     |                                |  |

### 2.2.2. Climate Data

To investigate the effect of climatic variables on the drought intensification rate, we calculated the monthly temperature and precipitation anomalies from the global gridded Climate Research Unit (CRU) TS 4.03 dataset by subtracting the climatology value. The dataset can be accessed at <https://www.uea.ac.uk/groups-and-centres/climatic-research-unit/data> (accessed on 27 March 2023). The spatial resolution of the data is  $0.5^\circ \times 0.5^\circ$ , and it spans from 1980 to 2018.

### 2.2.3. Vegetation Information

The vegetation condition used in the study was obtained from a daily vegetation index and phenological dataset (VIP), which was created using Advanced Very High-Resolution Radiometer (AVHRR) N07, N09, N11, and N14 datasets from 1981 to 1999 and Moderate Resolution Imaging Spectroradiometer (MODIS)/Terra MOD09 surface reflectance data from 2000 to 2014. It provides a long time series (34 years) of vegetation index and landscape phenological information and has been widely used in previous studies [23–29]. A two-step filtering approach for the input AVHRR and MODIS daily data was adopted to retain high-quality cloud-free data. Then, a hybrid per-pixel simple method based on the statistical correlation analysis across the two sensors (AVHRR and MODIS) was developed to correct the bias between them. Finally, spatial gaps were filled by temporal interpolation between the missing value and the closest available observations or from the long-term average record when the gaps persisted for periods longer than 3 months. More detail about the dataset can be found in the algorithm theoretical basis document from <https://lpdaac.usgs.gov/products/vip01v004/> (accessed on 27 March 2023). The normalized difference vegetation index (NDVI) in the VIP product was selected and resampled to a half degree and composited to a pentad scale similar to the RZSM ensemble dataset.

## 2.3. Methods

### 2.3.1. Drought Identification

In this study, droughts are defined by the deficit of the root zone soil moisture. We first identified all the drought events and then extracted the flash, general, and creep droughts according to different criteria. The drought identification was derived from the flash drought-detecting methodology proposed by Yuan et al. [30]. Specifically, a drought event was identified according to the following general rules:

- (1) The pentad-averaged root zone soil moisture decreases from above the 40th percentile to the 20th percentile;

- (2) If the soil moisture rises to the 25th percentile and continues for 5 pentads, the drought is considered to be demised;
- (3) The total duration of drought should not be less than 4 pentads (20 days).

The calculation of the percentile depends on a total of 40 RZSM values from the same pentad of history. Rule 1 defines the onset phase of the drought condition, that is, soil moisture changes from a normal or wet state to a dry state. Note that it is not required that the soil moisture percentile of the subsequent pentad be lower than that of the current pentad. As long as it is below the 40th, the drought is considered to be developing.

Different from Yuan's rules, we modified Rule 2 as that soil moisture should be equal to or above the 25th percentile for at least 6 pentads (1 month) to end the drought. Two reasons impelled us to make such a change: on the one hand, a too-short recovery time for soil moisture above the 25th percentile could lead to false recovery, after which drought might continue to develop (as seen in the example of the RZSM percentile at  $t + 14$  in Figure 2); on the other hand, when identifying drought events on a monthly scale, it is generally required that the time interval between two drought events should not less than one month. Rule 3 imposes a constraint on the drought duration since short-term droughts lasting less than 20 days are likely to have negligible environmental impacts.

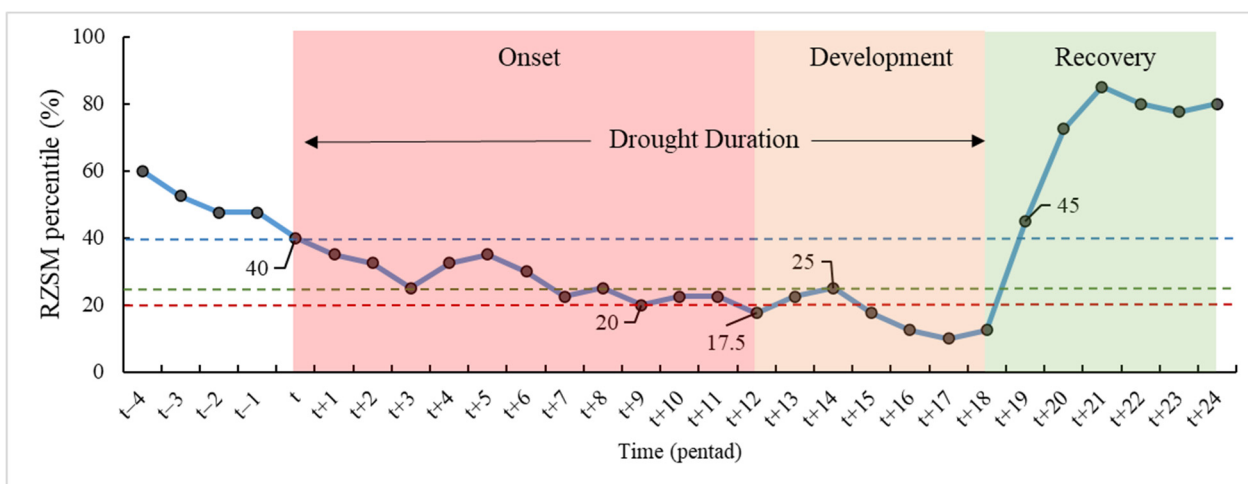


**Figure 2.** Schematic diagram of drought identification. The sample is located at 33.5°N, 70°E.

Then, we defined three types of droughts according to the mean decline rate and the length of the onset phase. These special events are considered a subset of drought, and their identification rules are as follows:

- (1) Flash drought: the length of RZSM changes in the onset phase should not exceed 5 pentads, which is equivalent to a maximum onset duration of 6 pentads (30 days), with the mean decline rate of no less than 5% in the RZSM percentiles for each pentad [30];
- (2) General drought: the length of onset phase exceeds 6 pentads but less than 12 pentads;
- (3) Creep drought: the length of onset phase exceeds 12 pentads; that is, more than 2 months.

### 2.3.2. Analysis of the Role of Climatic Variables and Drought's Ecological Impacts

Because the key to identifying the drought type is whether the soil water can drop from the 40th percentile to below the 20th percentile within 5 pentads (30 days in total), it is feasible to use the monthly data to analyze the climate anomaly differences at the onset timing of drought. If the drought occurs at the end of the month (26th or later), the climate data of the following month were used. To avoid the impact of the heavy precipitation at the end timing, we only chose the event that lasted longer than 7 pentads. Due to the number of creep droughts being much less than flash droughts, we used

the bootstrapping method, which takes 1000 values each time and repeats 2000 times to generate samples for three drought types, and the mean climate anomaly of 1000 values each time was calculated.

To evaluate the ecological impacts of three drought types, we followed several steps. Firstly, we calculated the NDVI anomaly by subtracting the historical averaged NDVI value, and then the z-score method was used to obtain the standardized NDVI anomaly series for each pentad. Next, we recorded the NDVI anomaly at the drought onset timing. For each SREX area and each drought type, the bootstrapping method, that is, sampling with a replacement, was also applied to generate samples from these recorded values. We sampled 1000 values each time and calculated the average. We repeated the sampling process 2000 times, obtaining 2000 samples for each drought type at the onset timing for further comparative analysis. We also extracted the vegetation conditions at the development timing ( $t + 12$  in Figure 2) and the end timing of drought ( $t + 18$  in Figure 2). Additionally, we calculated the vegetation degradation rate between the onset timing and the development timing using similar operations.

The flowchart of the study is given in Figure 3.

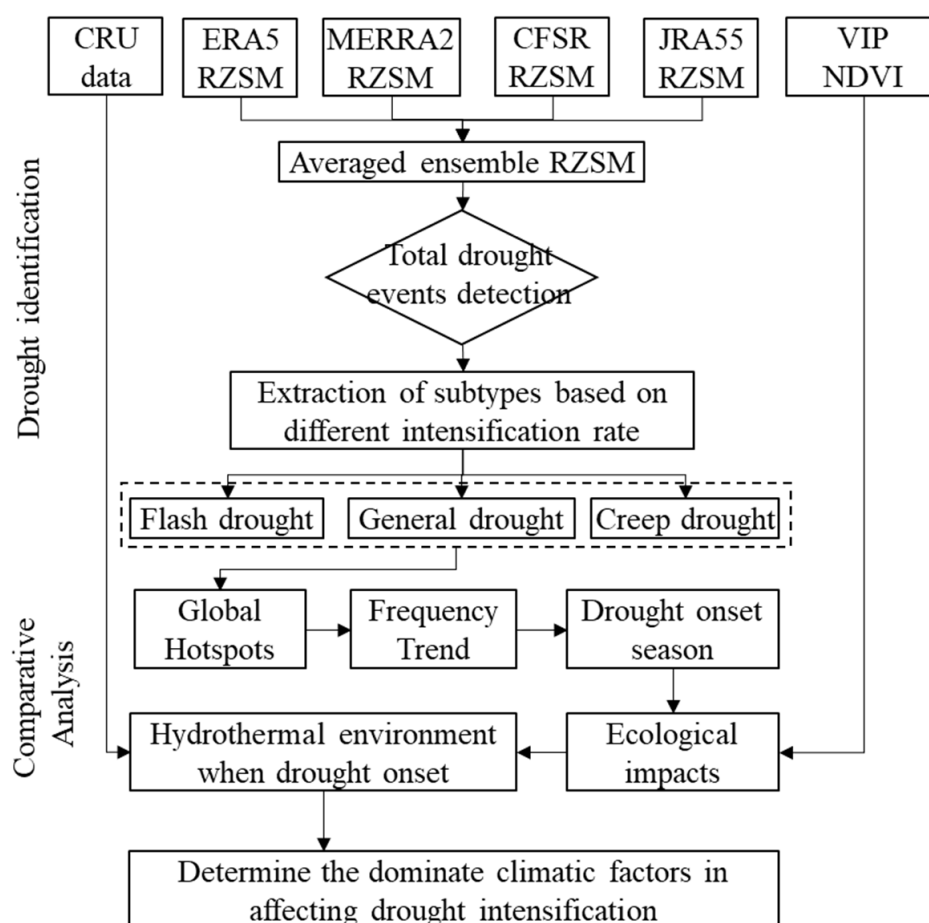


Figure 3. The flowchart of this study.

### 3. Results

#### 3.1. The Prevalence of Rapid Intensification over the Globe

The total drought events identified from the four reanalysis datasets and the ensemble dataset, without considering specific drought types, are presented first in Figure 4. Taking the neutral result provided by the ensemble dataset as a reference, JRA-55 generally overestimates the drought frequency over the globe, as well as ERA5, which overestimates in South America, and CFSR, which overestimates in Europe. However, consistencies can

still be found between the four reanalysis with at least three of the four datasets showing a high frequency of drought in eastern North America, Europe, South Asia, Southeast Asia, and southern China. From the perspective of latitudinal distribution, the four reanalysis datasets also show different peak positions. The peaks in the ERA5 results are located at high ( $60^{\circ}\text{N}$ ) and low ( $10^{\circ}\text{S}$ ) latitudes that more or less coincide with the CFSR results. MERRA2 and JRA-55 generally show similar patterns, with the peaks' location lower than the ERA5 and CFSR results. Significant differences in the total drought frequency over the past forty years imply large uncertainties between the datasets and highlight the importance of using an ensemble method with multiple datasets in the research. Therefore, we used the ensemble data to conduct the following analysis.

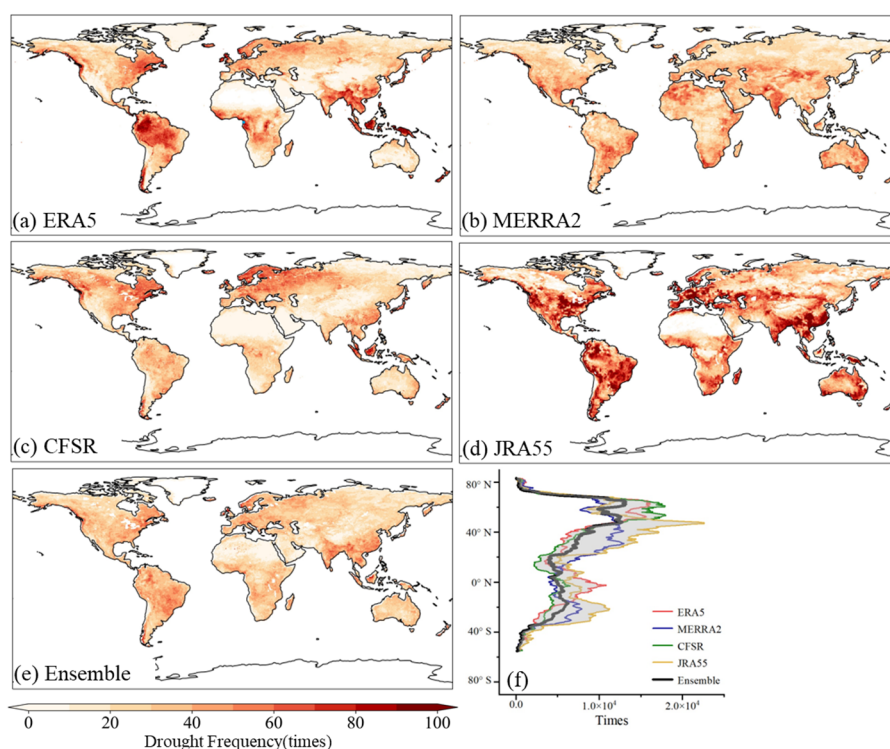


**Figure 4.** Spatial distributions of the accumulated drought frequency (unit: times) from 1980 to 2019 derived from ERA5 (a), MERRA2 (b), CFSR (c), JRA-55 (d), and the averaged ensemble (e). Latitudinal distribution is shown in (f).

According to the criteria mentioned in Section 2.2.1, the flash drought, general drought, and creep drought events were then extracted from the total drought events (Figure 5). Unlike the general drought and creep drought without spatial clustering over the globe (excluding Sahara), flash drought frequently happens in southern China, Southeast Asia, South Asia, eastern North America, South America, and parts of Europe and Africa. These hotspots are in close agreement with those regional studies that adopt similar RZSM-based methods, such as in Europe [31], Australia [32], and India [12]. Contrary to the previous common perception that flash droughts are rare events, they occur more frequently than the other two types. Some previous studies seem to provide similar evidence of frequent, rapid drops in soil moisture and high frequency of flash drought [12,16,33]; here, our results reinforce the conclusion that the rapid transition from an energy-limited to a water-limited condition is a prevalent phenomenon in most of the regions. Note that our definition of the flash drought was more restrictive than previous studies. We required a longer total duration of 4 pentads (20 days) and a longer recovery duration of 6 pentads to avoid a false recovery. Although the number of identified flash drought events can be limited by the maximum duration, e.g., no more than 18 pentads in the previous studies [8,12], the dominance of flash drought is not expected to change, as more than 60% of flash droughts

identified in our study still occur at a sub-seasonal scale (18 pentads) (please see later part Section 3.2).

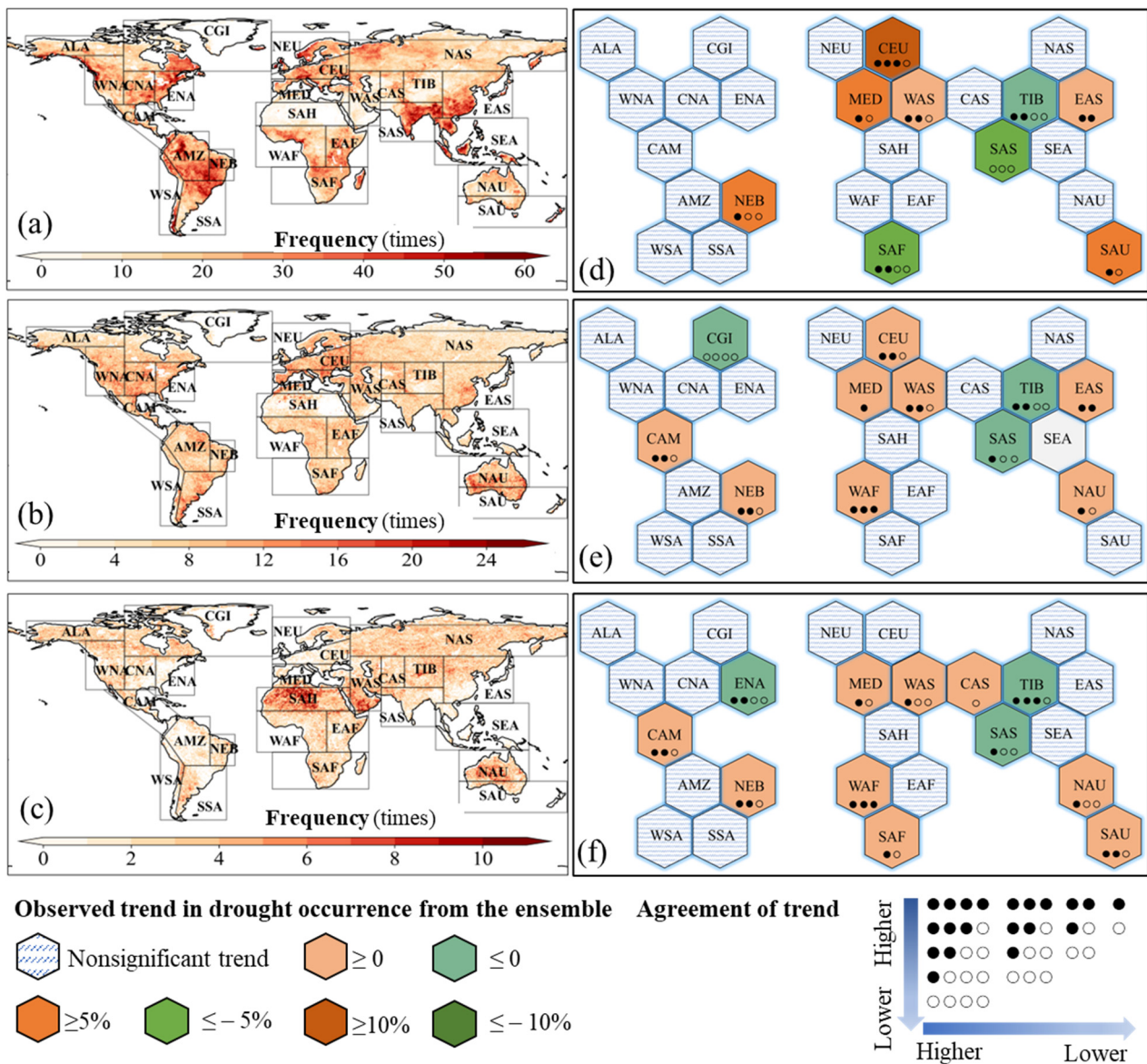


**Figure 5.** Spatial hotspots (left, unit: times) and frequency trends across the 26 IPCC-SREX climate divisions (right, unit: % decade<sup>-1</sup>) of flash drought (a,d), general drought (b,e), and creep drought (c,f) observed from the ensemble mean during 1980–2019. Only trends that passed the 95% confidence level are shown. The agreement of trend is based on assessing the trend from the individual ensemble members, and it is indicated by a combination of the number of filled or empty dots. One dot means the trend observed from a certain individual member shows a similar direction with the ensemble and filled or empty is determined by the confidence level (filled: greater than 95%).

Over the past forty years, flash drought has shown a significantly increased trend in frequency in the CEU, MED, WAS, EAS, SAU, and NEB regions, while a decreased trend in TIB, SAS, and SAF (Figure 5d). The agreements of frequency trends in these regions reach a moderate level, at least, as no less than two of the ensemble members (ERA5, MERRA2, CFSR, and JRA55) showed similar trends consistent with the ensemble dataset. Compared to flash drought, trends in the frequency of general drought (Figure 5e) and creep drought (Figure 5f) have been observed with a smaller changing rate but in wider regions; for example, both CAM, WAF, and NAU show an increasing trend, while CGI and ENA show

a decreasing trend. In addition, the agreements of the trends in general and creep drought frequency also reach a moderate level, except for the general drought trend in MED and the creep drought trend in CAS. Our results are the first to show trends in the global frequency of droughts at different intensification rates, with trends in flash droughts matching well with previous regional studies; for example, the increasing trend in CEU and MED [31], South Australia, and eastern South America, as well as the decreasing trend in India [7].

### 3.2. Characteristics of Drought Onset Duration and Total Duration

The frequency of flash drought is highly spatially correlated with the duration of their onset phase. Figure 6a shows that in flash drought hotspots, the onset duration is relatively shorter (about 2.5 pentads) than in other regions. No obvious spatial patterns in the onset duration are found for general drought, while for creep drought, the slowest onset duration is found in Central and North Asia and northern North America with more than 4 months (24 pentads) (Figure 6b,c). The regional statistical results also show similar patterns, as those flash droughts in SEA, SAS, SAF, NEB, and AMZ tend to develop faster than other regions, while creep droughts in ALA, CGI, EAS, and NAS develop more slowly (Figure 6d).

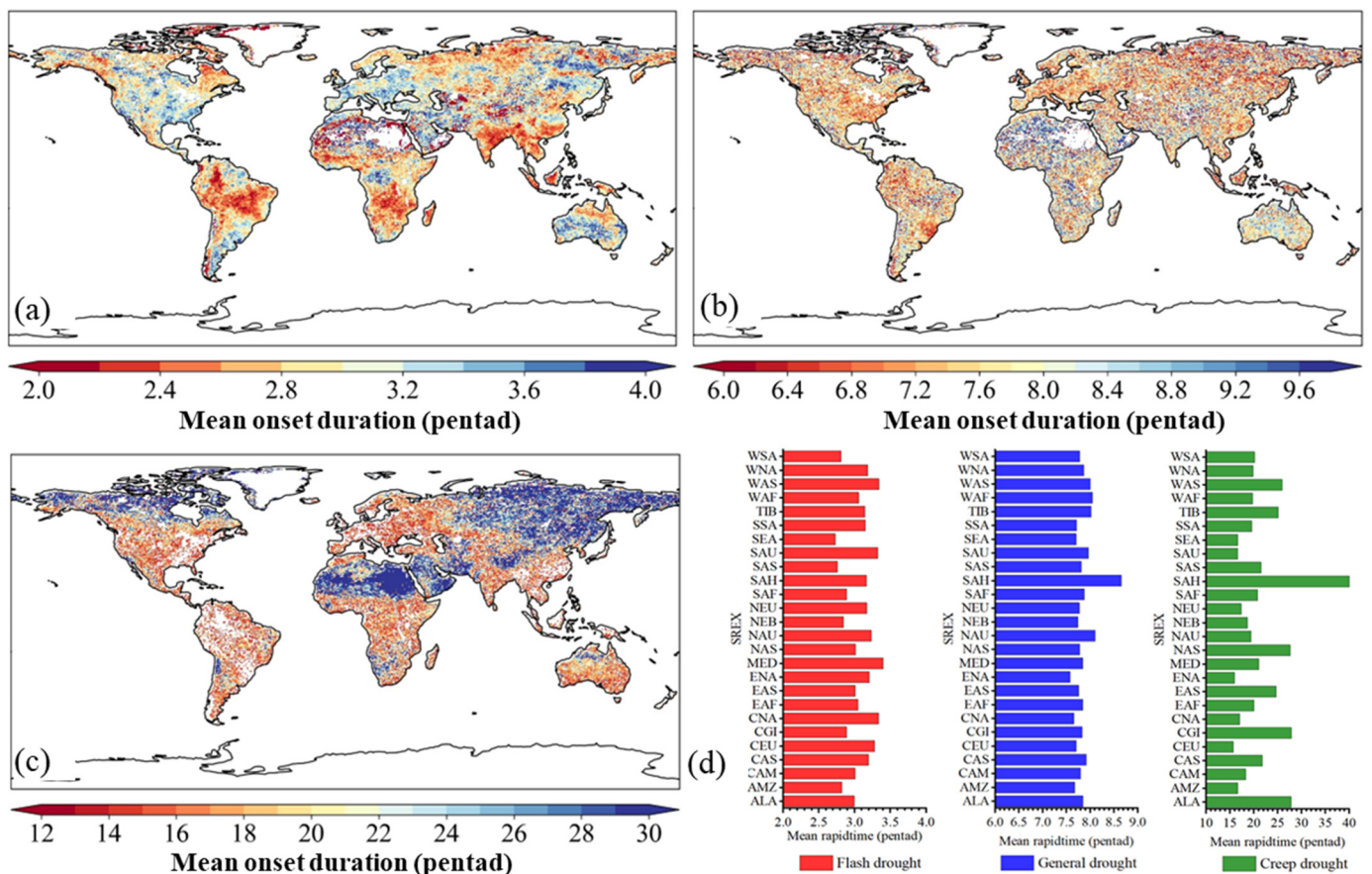


**Figure 6.** Spatial distribution of mean onset duration of flash drought (a), general drought (b), and creep drought (c), and the comparison of mean onset duration on a regional scale (d).

Flash drought generally has the shortest total duration compared with the other two drought types. Interestingly, the average total duration of the three drought types shows similar patterns: droughts in Central and North Asia and northern North America generally have the longest duration. This may be influenced by the temperate continental climate in these regions, which is good for the persistence of drought as the lower annual precipitation. The regional statistical results show that flash droughts are likely to end

within 3 months (the sub-seasonal scale) in all the regions (Figure 7d). With the drought type shifts from flash drought to creep drought, the total duration also increases gradually. As a result, less than 10% of creep droughts occur on a sub-seasonal scale. The difference in the total duration between regions also increases; for example, in the CEU, NEU, and ENA, creep droughts tend to last longer than 3 months but less than 6 months (seasonal scale) while in NAS, EAS, TIB, CGI, WAS, and ALA, etc., creep droughts are more likely to last above 6 months.

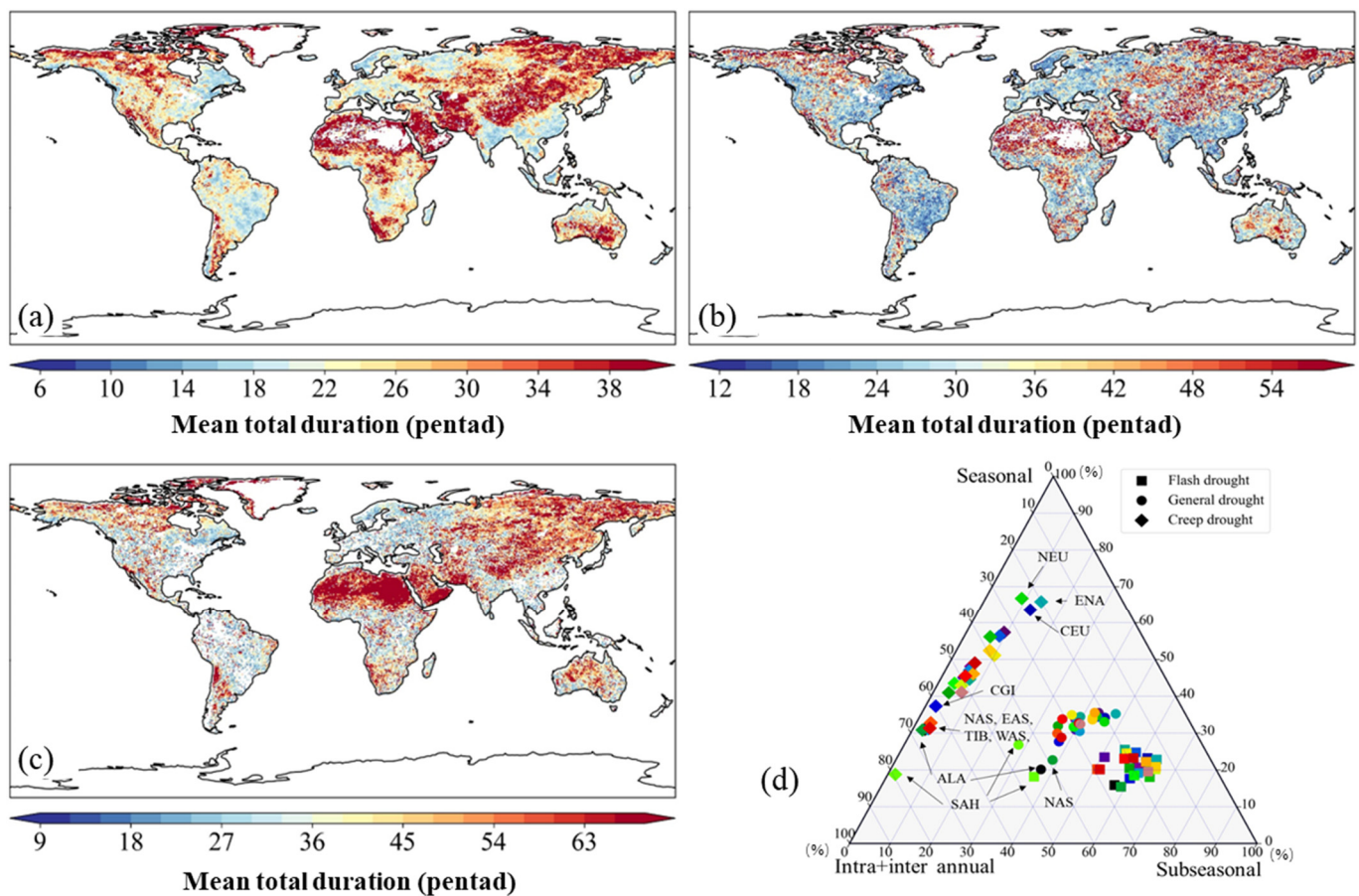


**Figure 7.** Similar to Figure 6 but for the mean total duration of flash drought (a), general drought (b), and creep drought (c). Each point in (d) represents a specific drought type for a region, and its position reflects how many events belonging to sub-seasonal (<3 months), seasonal (3–6 months), and intra-annual or inter-annual (>6 months), respectively.

### 3.3. Seasonality and Ecological Impacts

The distributions of the onset timing for flash drought, general drought, and creep drought were further compared across the 26 IPCC-SREX regions (Figure 8). Flash drought is somewhat similar to the features of compound warm-season droughts [34] as it mainly happens in the growing season. Many previous studies have also revealed this seasonality [7,12,16]. General drought can occur year-round as it shows little tendency in most regions, except for northern high latitudes with similar patterns to flash drought. The greatest difference in seasonality exists between flash drought and creep drought because creep drought is more likely to happen in the late or non-growing season, indicating the potential effect of climatic variables on the drought intensification rate.

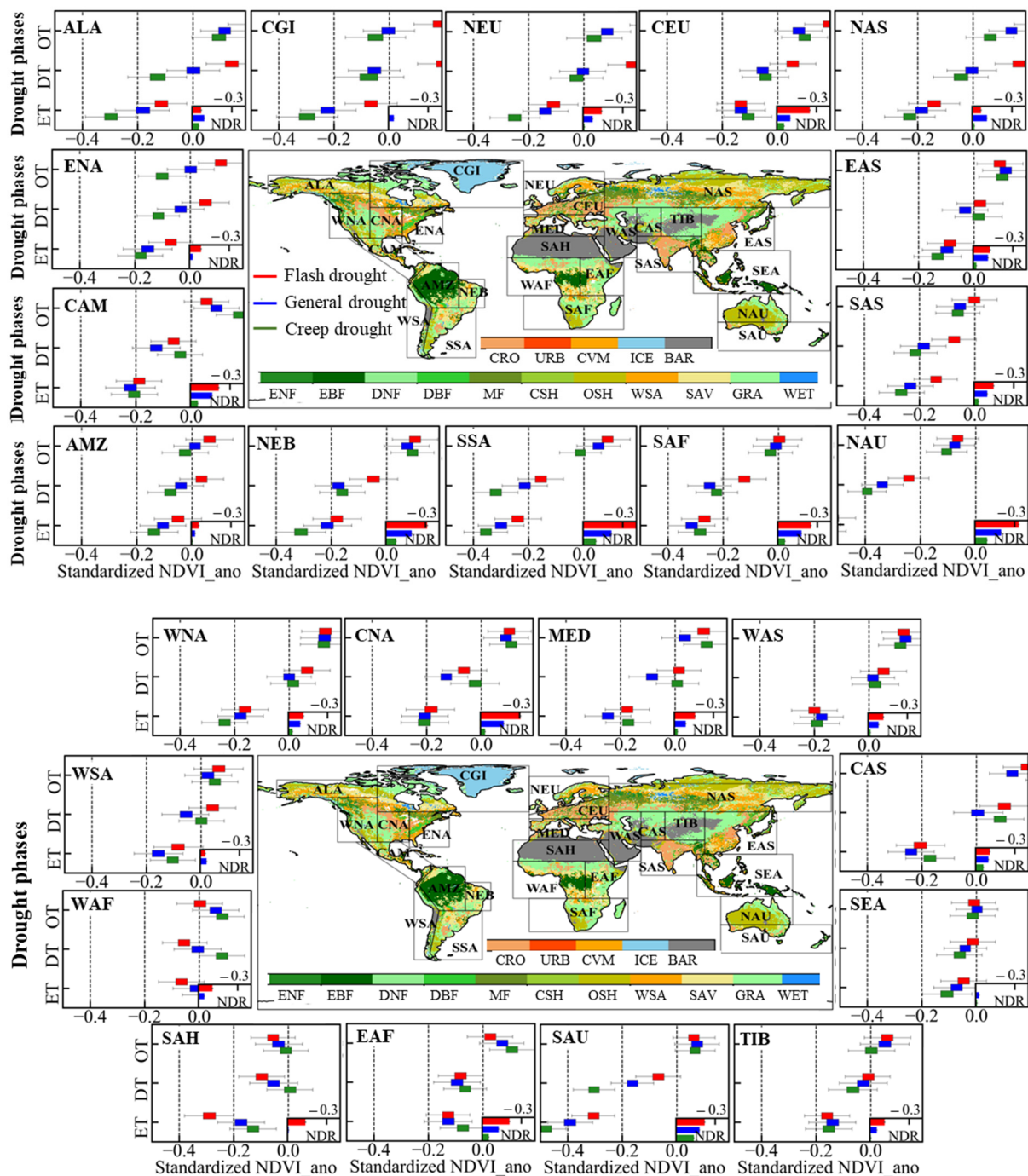


**Figure 8.** Ecological impacts of different drought types at onset timing (OT), development timing (DT), and drought end timing (ET) for parts of IPCC-SREX regions. For each boxplot, the inset at the upper left shows the probability of the month when droughts are most likely to happen, and the inset at the bottom right shows the mean decline rate of standardized NDVI anomaly (NDR, unit: % month<sup>-1</sup>) during the drought onset phase.

Our study is the first to reveal the seasonality difference between droughts with different intensification rates. Vegetations are expected to be more vulnerable to flash drought; however, creep droughts generally last to intra-annual (>6 months) or even inter-annual scales (>12 months) (Figure 7). Therefore, creep drought that occurs in winter may also have an impact on vegetation growth in the spring or summer of the following year. We further evaluated the vegetation condition that evolves during the drought (Figure 8).

The slightly improved vegetation condition at the onset timing of drought has been found at both global and regional scales. Compared with the other two drought types, the climate environment when flash drought occurs may promote vegetation growth more in most of the regions, especially in northern high latitudes (ALA, CGI, NEU, and NAS), where vegetation growth is mainly limited by energy. When the environment transfers into a water-limited condition, the response of vegetation varies from region and intensification rate. Vegetation generally shows a lag response to rapidly intensified water stress as its condition remains close to normal in most regions, especially in northern high latitudes, but it still shifts from a growing trend to a degradation trend. The lag response of vegetation is subtle to slowly intensified water stress, possibly because the longer onset duration is sufficient for vegetation to respond. As a result, greater vegetation degradation can be found in most of the regions at the end of the drought onset phase. However, vegetation degrades faster when suffering rapidly intensified drought. It should be noted that at the end of the drought, the slow onset drought generally resulted in more ecological losses because of the longer duration.

3.4. The Potential Effect of Precipitation and Temperature on the Intensification Rate

We further generated 1000 samples by the bootstrapping method for different drought types and compared the difference of the mean precipitation and temperature anomaly of these 1000 samples. Sampling was repeated 2000 times. The differences in precipitation (Figure 9a) and temperature (Figure 9b) anomalies between flash drought and general drought, as well as that between flash and creep droughts, answer how the climate affects the rate of drought intensification and their relative importance across the regions.

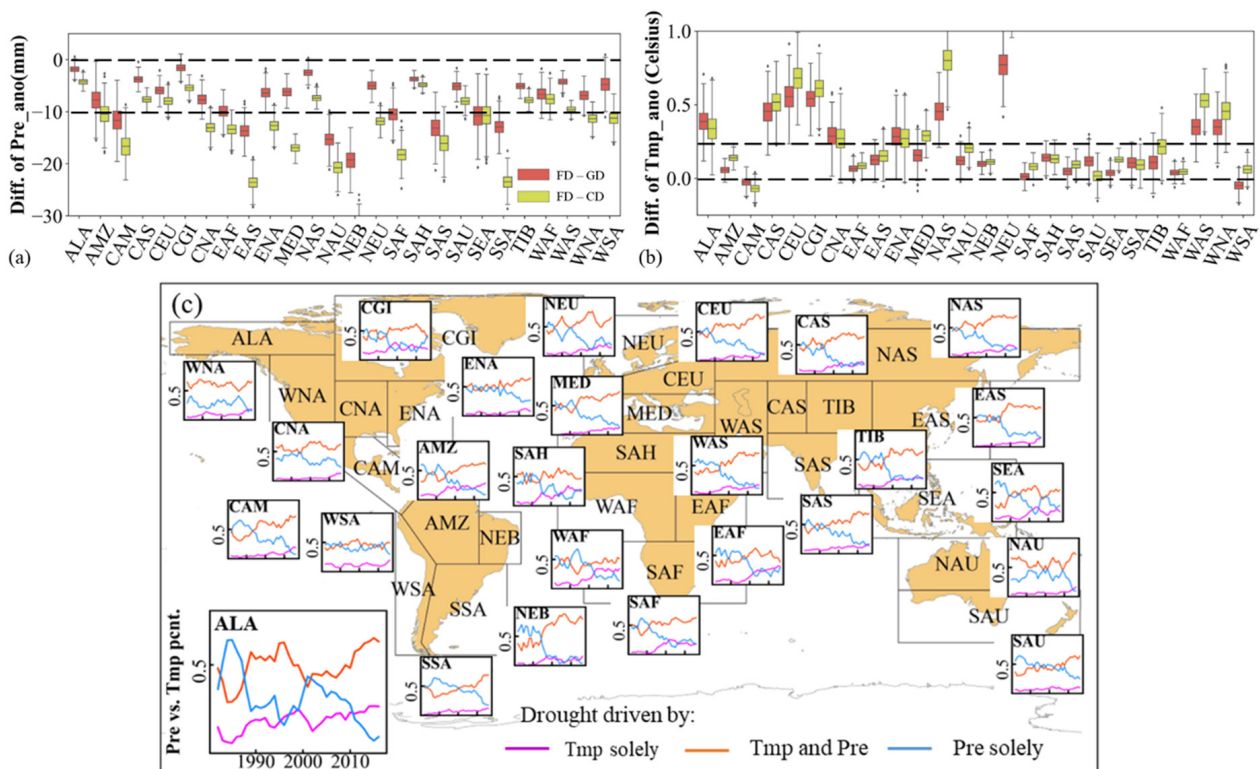


**Figure 9.** The difference in mean precipitation (a) and temperature (b) anomalies for the month when different droughts occurred. The red box in (a,b) shows the difference between flash drought and general drought while the yellow box shows that between flash drought and creep drought. (c) Contributions of the climatic variables associated with onset flash droughts are described as the percentage (pcnt.) of drought events per year driven by precipitation (Pre), temperature (Tmp), and both (Pre and Tmp).

Rapid onset drought generally happens in a relatively warmer and drier environment than that with slow onset ones, owing to the positive difference in temperature and negative difference in precipitation (Figure 8a,b). In most of the regions, the positive difference in temperature or negative difference of precipitation between flash drought and creep drought is much greater than that between flash and general, which indicates a generalized role of temperature (precipitation) as “the warmer (drier) the climate is, the faster the drought intensifies”. Interestingly, much higher precipitation differences but relatively lower temperature differences can be observed in the global monsoon-affected regions such as AMZ, CAM, NEB, SSA, EAF, SAF, NAU, SAS, EAS, and SEA, indicating the dominant role of precipitation in trigger flash drought. On the contrary, in midwestern Eurasia and high latitudes of the Northern Hemisphere, such as in ALA, CAS, CEU, CGI, NAS, NEU, and WAS, the role of temperature may be more prominent.

Another concern is whether the dominance of temperature or precipitation changes over time. We then divided the climate environment when flash drought occurs into three categories: dry and cold (precipitation anomaly < 0; temperature anomaly < 0), wet and hot (precipitation anomaly > 0; temperature anomaly > 0) and dry & hot (precipitation anomaly < 0; temperature anomaly > 0) [31]. The categories represent the flash drought driven by precipitation alone, temperature alone, and the collective effect of precipitation and temperature, respectively. We calculated the changes in the percentages of the three categories to investigate the dominance of temperature or precipitation changes over time. During the past 40 years, the increased contribution of temperature has been found in most of the regions, following an almost monotonic increase in the fraction of flash drought events, starting solely with high temperatures or the compound of high temperature and precipitation deficits. The most pronounced changes are observed in the tropics and northern high-latitude regions where the fraction of flash drought events solely driven by temperature slightly outlasts that by precipitation.

The observed increased contribution of temperature to flash drought responds to global warming. Previous research has reported the strong link between drought and temperature [35,36] and further attracted the attention of compound events of drought and heatwaves [37,38]. Recent studies have also demonstrated the important role of temperature in causing flash droughts, such as in China [30,39], southern Africa [40], and Brazil and Sahel [7]. The increased flash drought frequency in some regions could also be explained by rising temperatures; for example, more frequent heat waves in Europe [41–43]. It is reasonable to believe that under future climate scenarios, the main driver affecting the rate of drought intensification will gradually shift from precipitation to temperature in more regions.

#### 4. Discussion

It should be noted that the choice of drought identification methods would significantly affect the results of flash drought, in addition to the uncertainties brought by the datasets. Before we implemented the analysis work, we used the TCH (Three-cornered Hat) method to evaluate the uncertainties of the RZSM and ESR in the four reanalysis datasets to select the indicator with better performance. The RZSM and ESR are the two most popularly used variables in flash drought research [7–9,44]. The TCH is a simple and efficient way to evaluate the noise level in dataset/model simulations without relying on prior knowledge of the variables and has been widely used in the quality assessment of multi-source data, for example in the uncertainties estimation of GRACE TWS [45,46]. The uncertainty analysis for the four reanalysis datasets shows that MERRA2 performs best with the lowest relative uncertainties both in the RZSM and ESR among the four datasets, followed by ERA5 (Figure 10). Moreover, the uncertainties of RZSM between the four reanalysis datasets are generally much lower than that of the ESR, which is the main reason why we chose the RZSM but not the ESR in further analysis.

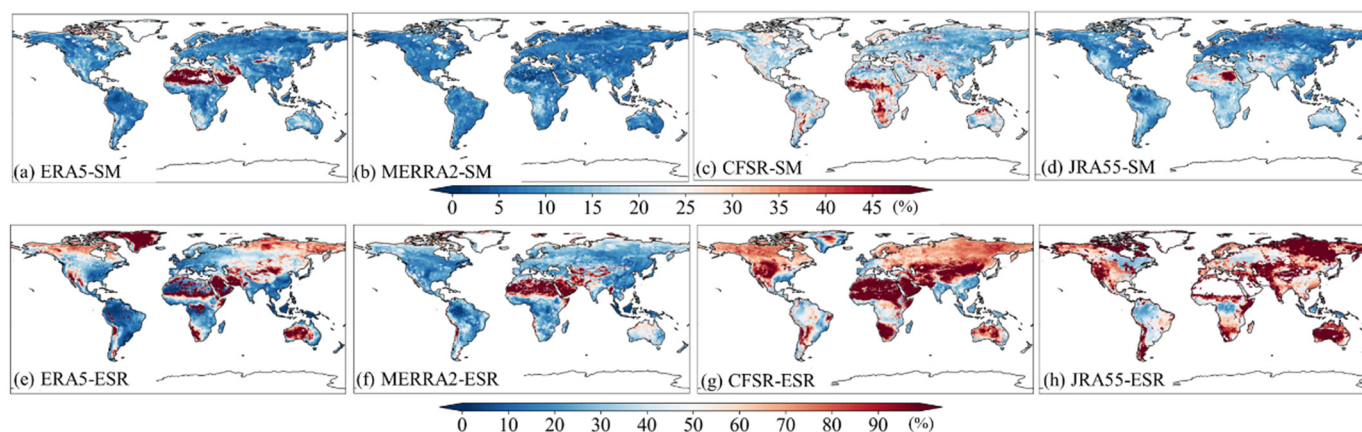


**Figure 10.** The relative uncertainties for the RZSM and ESR in ERA5, MERRA2, CFSR, and JRA55.

We introduced Yuan's [30] and Mishra's [8] definitions of flash drought to define two other types of drought, general drought and creep drought, based on the onset durations. The hotspots of flash drought we found are in high agreement with those regional studies that adopt similar RZSM-based methods, such as in Europe [31], Australia [32], and India [12]. Likewise, Mukherjee and Mishra [18] identified the global hotspots based on the new method, the MFDI (Multivariate Flash Drought Indicator), which is also consistent with our study. Moreover, even compared with the identification results based on the ESR variable, common hotspots can also be found, such as in South Asia, Southeast Asia, East Africa, and South America [7]. However, in some hotspots, flash drought can occur twice or even three times a year, leading to a debate about whether it can be considered a drought if the criterion is met so frequently. One undeniable fact is that the frequent, rapid changes in soil moisture evidenced by the rapid transitions from an energy-limited environment to a water-limited environment are part of the climatology of the locations at least [33].

From the perspective of climatic drivers, flash droughts are driven by extremely high temperatures or greater precipitation deficits (Figure 9). Precipitation and temperature act differently on the soil moisture decline. The persistent precipitation deficit for a period of time results in a decline in soil moisture, even with normal evaporation. Because of the land–atmosphere interaction, the declined soil moisture will lead to the warming of the atmospheric boundary layer and the increasing evaporation demand, which will further aggravate the decline of soil moisture. Compared to precipitation, extremely high temperatures will directly lead to a rapid decline of soil water by the increasing evaporation demand. It is noteworthy that vegetation also plays a role in propagating flash drought. Chen et al. [47] suggested that vegetation greening significantly increases the flash drought frequency in the Great Plains and the western United States during the warm seasons. The increased spring vegetation productivity leading to the fast depletion of SM in late spring and summer has also been found in Europe [48]. Therefore, the effect of vegetation growth on the drought intensification rate needs to be investigated in the future.

## 5. Conclusions

In this study, we defined three drought types, named flash drought, general drought, and creep drought, based on the mean decline rate of soil moisture during the drought onset phase, and a comparative analysis of the three drought types was implemented to assess the difference in global drought characteristics and ecological impact, and the relative contribution of the temperature and precipitation on the drought intensification rate.

Over the past 40 years, flash drought has occurred much more frequently than the other two types, which challenges our traditional perception that drought generally onsets slowly. Increased trends of drought frequency are found in midwestern Eurasia and sporadic regions in other continents. Compared to drought with slow intensification, the flash drought that mainly happens in the growing season generally causes faster but minor

vegetation deterioration. Through comparing climatic variable anomalies associated with drought onset, we find the roles of temperature and precipitation in regulating drought intensification rate as “the warmer (drier) the climate is, the faster the drought intensifies”; however, their dominance varies by region. Precipitation plays a dominant role mainly in the global monsoon regions, while in midwestern Eurasia and high latitudes of the Northern Hemisphere, the role of temperature is more prominent. What is alarming is that a monotonic increase in flash drought events driven by temperature is observed in most regions, which indicates that the contribution of temperature will be further enhanced in the future. Our findings advance the understanding of flash drought and can help policymakers and stakeholders develop more scientific policies in critical regions to minimize ecological and economic losses.

**Author Contributions:** J.H.: Conceptualization, Formal analysis, Investigation, Validation, Methodology, Writing—original draft, and Writing—review & editing. J.Z.: Conceptualization, Writing—review & editing, and Funding acquisition. S.Y.: Formal analysis and Writing—review & editing. A.M.S.: Writing—review & editing. All authors have read and agreed to the published version of the manuscript.

**Funding:** This work was supported by the Strategic Priority Research Program of the Chinese Academy of Sciences-A (No. XDA19030402), the Open Fund of Key Laboratory of Urban Land Resources Monitoring and Simulation, Ministry of Natural Resources (No. KF-2021-06-081), the Open Fund of the Key Laboratory of Urban Land Resources Monitoring and Simulation, Ministry of Land and Resources (No. KF-2016-02-026), the Natural Science Foundation of China (No. 42071425, No. 41871253), the National Key Research and Development Program of China (2020YFB1600103), the Natural Science Foundation of Shandong Province (No. ZR2020QE281), and the “Taishan Scholar” Project of Shandong Province (No. TSXZ201712).

**Data Availability Statement:** The RZSM datasets are provided by the ERA5 (European Center for Medium-Range Weather Forecasts Reanalysis 5, <https://cds.climate.copernicus.eu/cdsapp#!/dataset/reanalysis-era5-singlelevels?tab=form> (accessed on 27 March 2023)), the MERRA2 (Modern-Era Retrospective Analysis for Research and Applications, Version 2, <https://disc.gsfc.nasa.gov/datasets?project=MERRA-2> (accessed on 27 March 2023)), the CFSR (Climate Forecast System Reanalysis, <https://rda.ucar.edu/datasets/ds094.0/> (accessed on 27 March 2023)), and the JRA-55 (Japanese 55-year Reanalysis, <https://rda.ucar.edu/datasets/ds628.0/> (accessed on 27 March 2023)). Climate data are publicly available at the University of East Anglia’s Climatic Research Unit (<https://www.uea.ac.uk/groups-and-centres/climatic-research-unit/data> (accessed on 27 March 2023)). The vegetation condition dataset was obtained from <https://lpdaac.usgs.gov/products/vip01v004/> (accessed on 27 March 2023).

**Acknowledgments:** The authors are thankful for all the data providers.

**Conflicts of Interest:** We solemnly declare: this paper is our original work, and it has not been submitted to any other journal for publication and review, and there exists no conflict of interest in this manuscript’s submission.

## References

1. Mark, S.; Doug, L.; Mike, H.; Richard, H.; Karin, G.; Jim, A.; Brad, R.; Rich, T.; Mike, P.; David, S.; et al. The Drought Monitor. *Bull. Am. Meteorol. Soc.* **2002**, *83*, 1181–1190.
2. Mozny, M.; Trnka, M.; Zalud, Z.; Hlavinka, P.; Nekovar, J.; Potop, V.; Virag, M. Use of a soil moisture network for drought monitoring in the Czech Republic. *Theor. Appl. Climatol.* **2012**, *107*, 99–111. [[CrossRef](#)]
3. Yuan, X.; Ma, Z.G.; Pan, M.; Shi, C.X. Microwave remote sensing of short-term droughts during crop growing seasons. *Geophys. Res. Lett.* **2015**, *42*, 4394–4401. [[CrossRef](#)]
4. Gerken, T.; Bromley, G.T.; Ruddell, B.L.; Williams, S.; Stoy, P.C. Convective suppression before and during the United States Northern Great Plains flash drought of 2017. *Hydrol. Earth Syst. Sci.* **2018**, *22*, 4155–4163. [[CrossRef](#)]
5. Nguyen, H.; Wheeler, M.C.; Otkin, J.A.; Cowan, T.; Frost, A.; Stone, R. Using the evaporative stress index to monitor flash drought in Australia. *Environ. Res. Lett.* **2019**, *14*, 064016. [[CrossRef](#)]
6. Otkin, J.A.; Svoboda, M.; Hunt, E.D.; Ford, T.W.; Andersonson, M.C.; Hain, C.; Basara, J.B. FLASH DROUGHTS A Review and Assessment of the Challenges Imposed by Rapid-Onset Droughts in the United States. *Bull. Am. Meteorol. Soc.* **2018**, *99*, 911–919. [[CrossRef](#)]

7. Christian, J.I.; Basara, J.B.; Hunt, E.D.; Otkin, J.A.; Furtado, J.C.; Mishra, V.; Xiao, X.M.; Randall, R.M. Global distribution, trends, and drivers of flash drought occurrence. *Nat. Commun.* **2021**, *12*, 6330. [[CrossRef](#)]
8. Mishra, V.; Aadhar, S.; Mahto, S.S. Anthropogenic warming and intraseasonal summer monsoon variability amplify the risk of future flash droughts in India. *Npj Clim. Atmos. Sci.* **2021**, *4*, 1. [[CrossRef](#)]
9. Liu, Y.; Zhu, Y.; Zhang, L.; Ren, L.; Yuan, F.; Yang, X.; Jiang, S. Flash droughts characterization over China: From a perspective of the rapid intensification rate. *Sci. Total Environ.* **2020**, *704*, 135373. [[CrossRef](#)]
10. Nguyen, H.; Wheeler, M.C.; Hendon, H.H.; Lim, E.P.; Otkin, J.A. The 2019 flash droughts in subtropical eastern Australia and their association with large-scale climate drivers. *Weather Clim. Extrem.* **2021**, *32*, 100321. [[CrossRef](#)]
11. Osman, M.; Zaitchik, B.F.; Badr, H.S.; Christian, J.I.; Tadesse, T.; Otkin, J.A.; Anderson, M.C. Flash drought onset over the contiguous United States: Sensitivity of inventories and trends to quantitative definitions. *Hydrol. Earth Syst. Sci.* **2021**, *25*, 565–581. [[CrossRef](#)]
12. Mahto, S.S.; Mishra, V. Dominance of summer monsoon flash droughts in India. *Environ. Res. Lett.* **2020**, *15*, 104061. [[CrossRef](#)]
13. Poonia, V.; Goyal, M.K.; Jha, S.; Dubey, S. Terrestrial ecosystem response to flash droughts over India. *J. Hydrol.* **2022**, *605*, 127402. [[CrossRef](#)]
14. Mukherjee, S.; Mishra, A.K. Global Flash Drought Analysis: Uncertainties From Indicators and Datasets. *Earths Future* **2022**, *10*, e2022EF002660. [[CrossRef](#)]
15. Christian, J.I.; Basara, J.B.; Hunt, E.D.; Otkin, J.A.; Xiao, X. Flash drought development and cascading impacts associated with the 2010 Russian heatwave. *Environ. Res. Lett.* **2020**, *15*, 094078. [[CrossRef](#)]
16. Chen, L.G.; Gottschalck, J.; Hartman, A.; Miskus, D.; Tinker, R.; Artusa, A. Flash Drought Characteristics Based on US Drought Monitor. *Atmosphere* **2019**, *10*, 498. [[CrossRef](#)]
17. Noguera, I.; Vicente-Serrano, S.M.; Dominguez-Castro, F. The Rise of Atmospheric Evaporative Demand Is Increasing Flash Droughts in Spain During the Warm Season. *Geophys. Res. Lett.* **2022**, *49*, e2021GL097703. [[CrossRef](#)]
18. Mukherjee, S.; Mishra, A.K. A Multivariate Flash Drought Indicator for Identifying Global Hotspots and Associated Climate Controls. *Geophys. Res. Lett.* **2022**, *49*, e2021GL096804. [[CrossRef](#)]
19. Mo, K.C.; Lettenmaier, D.P. Heat wave flash droughts in decline. *Geophys. Res. Lett.* **2015**, *42*, 2823–2829. [[CrossRef](#)]
20. Mo, K.C.; Lettenmaier, D.P. Precipitation Deficit Flash Droughts over the United States. *J. Hydrometeorol.* **2016**, *17*, 1169–1184. [[CrossRef](#)]
21. Liu, Y.; Zhu, Y.; Ren, L.; Otkin, J.; Hunt, E.D.; Yang, X.; Yuan, F.; Jiang, S. Two Different Methods for Flash Drought Identification: Comparison of Their Strengths and Limitations. *J. Hydrometeorol.* **2020**, *21*, 691–704. [[CrossRef](#)]
22. Zhang, Y.; Liu, X.H.; Jiao, W.Z.; Zhao, L.J.; Zeng, X.M.; Xing, X.Y.; Zhang, L.N.; Hong, Y.X.; Lu, Q.Q. A new multi-variable integrated framework for identifying flash drought in the Loess Plateau and Qinling Mountains regions of China. *Agric. Water Manag.* **2022**, *265*, 107544. [[CrossRef](#)]
23. Didan, K. Multi-satellite earth science data record for studying global vegetation trends and changes. In Proceedings of the 2010 International Geoscience and Remote Sensing Symposium, Honolulu, HI, USA, 25–30 July 2010; p. 2530.
24. Dass, P.; Rawlins, M.A.; Kimball, J.S.; Kim, Y. Environmental controls on the increasing GPP of terrestrial vegetation across northern Eurasia. *Biogeosciences* **2016**, *13*, 45–62. [[CrossRef](#)]
25. Marshall, M.; Okuto, E.; Kang, Y.; Opiyo, E.; Ahmed, M. Global assessment of Vegetation Index and Phenology Lab (VIP) and Global Inventory Modeling and Mapping Studies(GIMMS) version 3 products. *Biogeosciences* **2016**, *13*, 625–639. [[CrossRef](#)]
26. Chen, X.; Yang, Y. Observed earlier start of the growing season from middle to high latitudes across the Northern Hemisphere snow-covered landmass for the period 2001–2014. *Environ. Res. Lett.* **2020**, *15*, 034042. [[CrossRef](#)]
27. Helman, D.; Zaitchik, B.F.; Funk, C. Climate has contrasting direct and indirect effects on armed conflicts. *Environ. Res. Lett.* **2020**, *15*, 104017. [[CrossRef](#)]
28. Wu, M.; Vico, G.; Manzoni, S.; Cai, Z.; Bassiouni, M.; Tian, F.; Zhang, J.; Ye, K.; Messori, G. Early growing season anomalies in vegetation activity determine the large-scale climate-vegetation coupling in Europe. *J. Geophys. Res. Biogeosci.* **2021**, *126*, e2020JG006167. [[CrossRef](#)]
29. Yin, C.; Yang, Y.; Yang, F.; Chen, X.; Xin, Y.; Luo, P. Diagnose the dominant climate factors and periods of spring phenology in Qinling Mountains, China. *Ecol. Indic.* **2021**, *131*, 108211. [[CrossRef](#)]
30. Yuan, X.; Wang, L.; Wu, P.; Ji, P.; Sheffield, J.; Zhang, M. Anthropogenic shift towards higher risk of flash drought over China. *Nat. Commun.* **2019**, *10*, 4661. [[CrossRef](#)]
31. Shah, J.; Hari, V.; Rakovec, O.; Markonis, Y.; Samaniego, L.; Mishra, V.; Hanel, M.; Hinz, C.; Kumar, R. Increasing footprint of climate warming on flash droughts occurrence in Europe. *Environ. Res. Lett.* **2022**, *17*, 064017. [[CrossRef](#)]
32. Parker, T.; Gallant, A.; Hobbins, M.; Hoffmann, D. Flash drought in Australia and its relationship to evaporative demand. *Environ. Res. Lett.* **2021**, *16*, 064033. [[CrossRef](#)]
33. Lisonbee, J.; Ribbe, J.; Otkin, J.A.; Pudmenzky, C. Wet season rainfall onset and flash drought: The case of the northern Australian wet season. *Int. J. Climatol.* **2022**, *42*, 6499–6514. [[CrossRef](#)]
34. Markonis, Y.; Kumar, R.; Hanel, M.; Rakovec, O.; Maca, P.; AghaKouchak, A. The rise of compound warm-season droughts in Europe. *Sci. Adv.* **2021**, *7*, eabb9668. [[CrossRef](#)]
35. Griffin, D.; Anchukaitis, K.J. How unusual is the 2012–2014 California drought? *Geophys. Res. Lett.* **2014**, *41*, 9017–9023. [[CrossRef](#)]

36. Williams, A.P.; Cook, E.R.; Smerdon, J.E.; Cook, B.I.; Abatzoglou, J.T.; Bolles, K.; Baek, S.H.; Badger, A.M.; Livneh, B. Large contribution from anthropogenic warming to an emerging North American megadrought. *Science* **2020**, *368*, 314–318. [[CrossRef](#)]
37. Kong, Q.; Guerreiro, S.B.; Blenkinsop, S.; Li, X.-F.; Fowler, H.J. Increases in summertime concurrent drought and heatwave in Eastern China. *Weather Clim. Extrem.* **2020**, *28*, 100242. [[CrossRef](#)]
38. Mukherjee, S.; Mishra, A.K. Increase in Compound Drought and Heatwaves in a Warming World. *Geophys. Res. Lett.* **2021**, *48*, e2020GL090617. [[CrossRef](#)]
39. Wang, Y.M.; Yuan, X. Anthropogenic Speeding Up of South China Flash Droughts as Exemplified by the 2019 Summer-Autumn Transition Season. *Geophys. Res. Lett.* **2021**, *48*, e2020GL091901. [[CrossRef](#)]
40. Yuan, X.; Wang, L.; Wood, E.F. Anthropogenic intensification of southern african flash droughts as exemplified by the 2015/16 season. *Bull. Am. Meteorol. Soc.* **2018**, *99*, S86–S90. [[CrossRef](#)]
41. Christidis, N.; Jones, G.S.; Stott, P.A. Dramatically increasing chance of extremely hot summers since the 2003 European heatwave. *Nat. Clim. Chang.* **2015**, *5*, 46–50. [[CrossRef](#)]
42. Bras, T.A.; Seixas, J.; Carvalhais, N.; Jagermeyr, J. Severity of drought and heatwave crop losses tripled over the last five decades in Europe. *Environ. Res. Lett.* **2021**, *16*, 065012. [[CrossRef](#)]
43. Pflleiderer, P.; Schleussner, C.F.; Kornhuber, K.; Coumou, D. Summer weather becomes more persistent in a 2 degrees C world. *Nat. Clim. Chang.* **2019**, *9*, 666–671. [[CrossRef](#)]
44. Koster, R.D.; Schubert, S.D.; Wang, H.; Mahanama, S.P.; DeAngelis, A.M. Flash Drought as Captured by Reanalysis Data: Disentangling the Contributions of Precipitation Deficit and Excess Evapotranspiration. *J. Hydrometeorol.* **2019**, *20*, 1241–1258. [[CrossRef](#)]
45. Ferreira, V.; Montecino, H.D.C.; Yakubu, C.; Heck, B. Uncertainties of the Gravity Recovery and Climate Experiment time-variable gravity-field solutions based on three-cornered hat method. *J. Appl. Remote Sens.* **2016**, *10*, 015015. [[CrossRef](#)]
46. Long, D.; Pan, Y.; Zhou, J.; Chen, Y.; Hou, X.Y.; Hong, Y.; Scanlon, B.R.; Longueyergne, L. Global analysis of spatiotemporal variability in merged total water storage changes using multiple GRACE products and global hydrological models. *Remote Sens. Environ.* **2017**, *192*, 198–216. [[CrossRef](#)]
47. Chen, L.; Ford, T.W.; Yadav, P. The Role of Vegetation in Flash Drought Occurrence: A Sensitivity Study Using Community Earth System Model, Version 2. *J. Hydrometeorol.* **2021**, *22*, 845–857. [[CrossRef](#)]
48. Bastos, A.; Ciais, P.; Friedlingstein, P.; Sitch, S.; Pongratz, J.; Fan, L.; Wigneron, J.P.; Weber, U.; Reichstein, M.; Fu, Z.; et al. Direct and seasonal legacy effects of the 2018 heat wave and drought on European ecosystem productivity. *Sci. Adv.* **2020**, *6*, eaba2724. [[CrossRef](#)]

**Disclaimer/Publisher’s Note:** The statements, opinions and data contained in all publications are solely those of the individual author(s) and contributor(s) and not of MDPI and/or the editor(s). MDPI and/or the editor(s) disclaim responsibility for any injury to people or property resulting from any ideas, methods, instructions or products referred to in the content.